J|A|C|S
ARTICLES
Published on Web 02/26/2005

The Binding Energy of Two Nitrilotriacetate Groups Sharing a Nickel Ion

David Tareste,[†] Frédéric Pincet,[†] Marie Brellier,[‡] Charles Mioskowski,[‡] and Éric Perez*[,†]

Contribution from the Laboratoire de Physique Statistique de l'Ecole Normale Supérieure, 24, rue Lhomond, 75005 Paris, France, and Laboratoire de Synthèse Bio-Organique, Faculté de Pharmacie, 74, Route du Rhin, 67401 Illkirch, France

Received October 26, 2004; E-mail: perez@lps.ens.fr

Abstract: Among the various molecular interactions used to construct supramolecular self-assembling systems, homoliganded metallic NTA−Ni−NTA complexes have received little attention despite their considerable potential applications, such as the connection of different biochemical functions. The stability of this complex is investigated here by using two concordant nanotechniques (surface forces apparatus and vesicle micromanipulation) that allow direct measurements of adhesion energies due to the chelation of nickel ions by nitrilotriacetate (NTA) groups grafted on surfaces. We show that two NTA groups can share a nickel ion, and that the association of a Ni−NTA complex with an NTA group has a molecular binding energy of 1.4 kcal/mol. Binding measurements in bulk by isothermal titration calorimetry experiments give the same value and, furthermore, indicate that the Ni−NTA chelation bond is about five times stronger than the NTA−Ni−NTA one. This first direct proof and quantification of the simultaneous chelation of a nickel ion by two NTA groups sheds new light on association dynamics involving chelation processes and offers perspectives for the development of new supramolecular assemblies and anchoring strategies.

Introduction

Supramolecular self-assembling systems are generally based on noncovalent cooperative interactions which permit the construction of highly sophisticated structures presenting tailored functions.[1−3] The weak interactions involved in these systems include hydrophobic interactions, hydrogen bonding, π-stacking interactions, metal coordination bonding, and specific ligand−receptor interactions. One of the major goals in supramolecular chemistry is to control the structure and dynamic of matter through self-organization. This includes a characterization, at the molecular level, of the interactions that hold the building blocks together. Recent advances in nanoscale force and adhesion measurements have already allowed the quantification of hydrogen bonding interactions,[4,5] but many other weak interactions, such as metal−ligand binding, remain poorly described.

Heteroliganded metallic complexes have received considerable attention during the past few years since genetically engineered His-tagged proteins were found to bind specifically to Ni−NTA moieties, thus forming a His−Ni−NTA ternary complex. Today, such a complex is extensively used for purification purposes, surface functionalization by proteins, and bidimensional crystallization through Ni−NTA functionalized lipids.[6−11] Homoliganded metallic complexes, such as metal−bis(carboxylate),[12,13] metal−bis(phosphonate),[14,15] and metal−bis(terpyridine),[16−18] have also been used to generate supramolecular systems with original structures and novel optical, electric, or magnetic properties. Many potential applications could be derived from the formation of NTA−Ni−NTA

[†] Laboratoire de Physique Statistique de l'Ecole Normale Supérieure.
[‡] Laboratoire de Synthèse Bio-Organique.

(1) Whitesides, G. M.; Mathias, J. P.; Seto, C. T. *Science* **1991**, *254*, 1312−1319.
(2) Lehn, J. M. *Science* **2002**, *295*, 2400−2403.
(3) Dmitriev, A.; Spillmann, H.; Lin, N.; Barth, J. V.; Kern, K. *Angew. Chem., Int. Ed.* **2003**, *42*, 2670−2673.
(4) Pincet, F.; Perez, E.; Bryant, G.; Lebeau, L.; Mioskowski, C. *Phys. Rev. Lett.* **1994**, *73*, 2780−2783.
(5) Tareste, D.; Pincet, F.; Perez, E.; Rickling, S.; Mioskowski, C.; Lebeau, L. *Biophys. J.* **2002**, *83*, 3675−3681.
(6) Hochuli, E.; Bannwarth, W.; Dobeli, H.; Gentz, R.; Stuber, D. *Biotechnology* **1988**, *6*, 1321−1325.
(7) Schmitt, L.; Dietrich, C.; Tampe, R. *J. Am. Chem. Soc.* **1994**, *116*, 8485−8491.
(8) Venien-Bryan, C.; Balavoine, F.; Toussaint, B.; Mioskowski, C.; Hewat, E. A.; Helme, B.; Vignais, P. M. *J. Mol. Biol.* **1997**, *274*, 687−692.
(9) Wilson-Kubalek, E. M.; Brown, R. E.; Celia, H.; Milligan, R. A. *Proc. Natl. Acad. Sci. U.S.A.* **1998**, *95*, 8040−8045.
(10) Bischler, N.; Balavoine, F.; Milkereit, P.; Tschochner, H.; Mioskowski, C.; Schultz, P. *Biophys. J.* **1998**, *74*, 1522−1532.
(11) Lebeau, L.; Lach, F.; Venien-Bryan, C.; Renault, A.; Dietrich, J.; Jahn, T.; Palmgren, M. G.; Kuhlbrandt, W.; Mioskowski, C. *J. Mol. Biol.* **2001**, *308*, 639−647.
(12) Guo, S. W.; Konopny, L.; Popovitz-Biro, R.; Cohen, H.; Porteanu, H.; Lifshitz, E.; Lahav, M. *J. Am. Chem. Soc.* **1999**, *121*, 9589−9598.
(13) Waggoner, T. A.; Last, J. A.; Kotula, P. G.; Sasaki, D. Y. *J. Am. Chem. Soc.* **2001**, *123*, 496−497.
(14) Cao, G.; Hong, H. G.; Mallouk, T. E. *Acc. Chem. Res.* **1992**, *25*, 420−427.
(15) Benitez, I. O.; Bujoli, B.; Camus, L. J.; Lee, C. M.; Odobel, F.; Talham, D. R. *J. Am. Chem. Soc.* **2002**, *124*, 4363−4370.
(16) Liang, Y. W.; Schmehl, R. H. *J. Chem. Soc., Chem. Commun.* **1995**, 1007−1008.
(17) Constable, E. C.; Meier, W.; Nardin, C.; Mundwiler, S. *Chem. Commun.* **1999**, 1483−1484.
(18) Lohmeijer, B. G. G.; Schubert, U. S. *Angew. Chem., Int. Ed.* **2002**, *41*, 3825−3829.

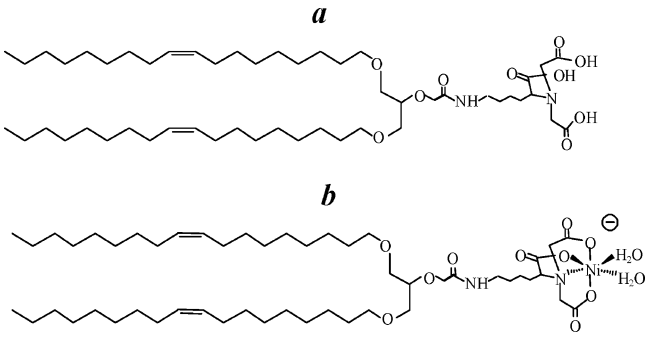

Figure 1. Structure of the synthesized lipids: (a) NTA−DOGA and (b) Ni−NTA−DOGA. The unsaturations of the chains allow the functionalized lipids to have some translational freedom within their monolayer, and the flexible spacers provide rotational freedom to the headgroups. Functional groups from opposite surfaces can thus adopt the most favorable configuration to interact with each other.

complexes, which up to now have been scarcely studied. Since it involves only small synthetic molecules, this system would be notably more convenient than the usual streptavidin−biotin interaction for anchoring specific molecules on surfaces or creating bifunctional compounds.

The present paper is devoted to the evaluation of the stability of NTA−Ni−NTA complexes on surfaces by using the surface forces apparatus[19] and the vesicle micromanipulation technique[20−22] and, in bulk, through isothermal titration calorimetry experiments.[23] The first two techniques involved bilayers in which lipids having either the NTA ligand or its chelate, the Ni−NTA complex, as headgroups were incorporated (NTA−DOGA and Ni−NTA−DOGA lipids, Figure 1). SFA experiments involved monolayers of NTA−DOGA or Ni−NTA−DOGA lipids deposited by the Langmuir−Blodgett method[24] on solid mica surfaces, with their headgroups facing the aqueous medium (Figure 2a). In the vesicle micromanipulation experiments, NTA−DOGA or Ni−NTA−DOGA lipids were incorporated in the membrane of stearoyl−oleoyl−phosphatidyl−choline (SOPC) giant vesicles in the molar ratio of 1:10 (1 molecule of NTA−DOGA or Ni−NTA−DOGA for 10 molecules of SOPC) (Figure 3a). All of the experiments were performed at a pH value close to physiological pH with tris(hydroxymethyl)aminomethane (Tris) buffer (pH 8.0). Surface forces apparatus and vesicle micromanipulation experiments gave concordant results; two NTA groups can dimerize by sharing a nickel ion, and the corresponding binding energy is weak (about 1.4 kcal/mol). Complementary microcalorimetry experiments were performed in volume by the titration of an aqueous solution of $NiCl_2$ with NTA groups. They led to the bulk determination of Ni−NTA and NTA−Ni−NTA association constants and chelation bond energies. The value obtained for the energy of the NTA−Ni−NTA complex shows no significant difference with the one measured on surface. Furthermore, the Ni−NTA chelation bond was found to be five times stronger (6.5 kcal/mol) than the NTA−Ni−NTA one. These results suggest that NTA−Ni−NTA complexes are stabilized by weak interactions and are, therefore, a promising tool for the development of novel dynamic supramolecular assemblies.

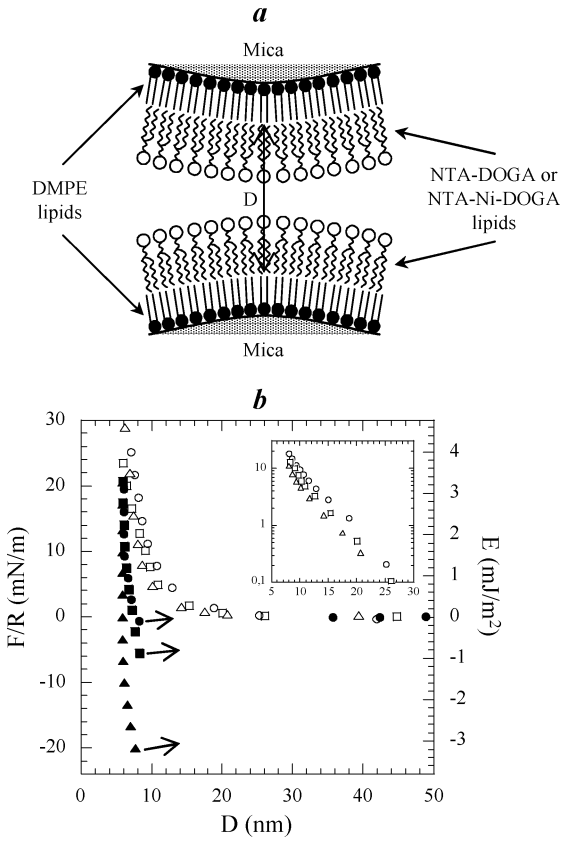

Figure 2. (a) SFA experiments. The reference distance $D = 0$ corresponds to the contact between DMPE hydrophobic tails. NTA−DOGA and Ni−NTA−DOGA lipids form fluid layers even at high surface pressure, as checked from their compression isotherm. Their stability relative to desorption was measured at both the air/Tris and mica/Tris interfaces and proved to be less than 1%/h. This ensures that the lipids form stable, close-packed, and fluid monolayers on the time scale of force measurement experiments. (b) Force−distance profiles of the three systems (NTA/NTA, circles; NTA/Ni−NTA, squares, and Ni−NTA/Ni−NTA, triangles; approaching phases, open symbols; separating phases, filled symbols). Adhesive jumps are highlighted by arrows. The inset shows in a semilog scale the electrostatic double-layer repulsion that occurs between charged NTA−DOGA or Ni−NTA−DOGA monolayers.

Materials and Methods

Chemicals. The synthesis of the functionalized lipids (Figure 1) has been described in detail elsewhere.[10] In brief, the NTA group was covalently bound to two unsaturated C_{18} alkyl chains via a flexible spacer, thus leading to the desired lipid, 2-(biscarboxymethylamino)-6-[2-(1,3-di-*O*-oleylglyceroxy)acetylamino] hexanoic acid lipid (NTA−DOGA lipid). To obtain the Ni−NTA−DOGA lipid, a chloroform solution of the NTA−DOGA lipid was stirred with an aqueous buffer (pH 8) containing 1 equiv of $NiCl_2$.

Dimyristoyl−phosphatidyl−ethanolamine (DMPE) and SOPC lipids were purchased from Avanti Polar lipids. Tris buffer was purchased from Merck-Eurolab. All experiments were made using ultrapure water (purified with the Elgastat Maxima system, HPLC model).

Surface Forces Apparatus (SFA). The SFA technique gives the force (F) as a function of the separation distance (D) between two crossed-cylinder surfaces (radius R). The ratio of $F(D)/R$ is proportional to the interaction energy $E(D)$ between two plane surfaces following the Derjaguin approximation:[25]

$$\frac{F(D)}{R} = 2\pi E(D) \qquad (1)$$

(19) Israelachvili, J. N.; Adams, G. E. *J. Chem. Soc., Faraday Trans. 1* **1978**, *74*, 975−1001.
(20) Evans, E. *Biophys. J.* **1980**, *31*, 425−431.
(21) Evans, E.; Metcalfe, M. *Biophys. J.* **1984**, *46*, 423−426.
(22) Evans, E. *Colloids Surf.* **1990**, *43*, 327−347.
(23) Heerklotz, H.; Seelig, J. *Biochim. Biophys. Acta* **2000**, *1508*, 69−85.
(24) Gaines, G. L. *Insoluble Monolayers at Liquid−Gas Interfaces*; Interscience: New York, 1991.

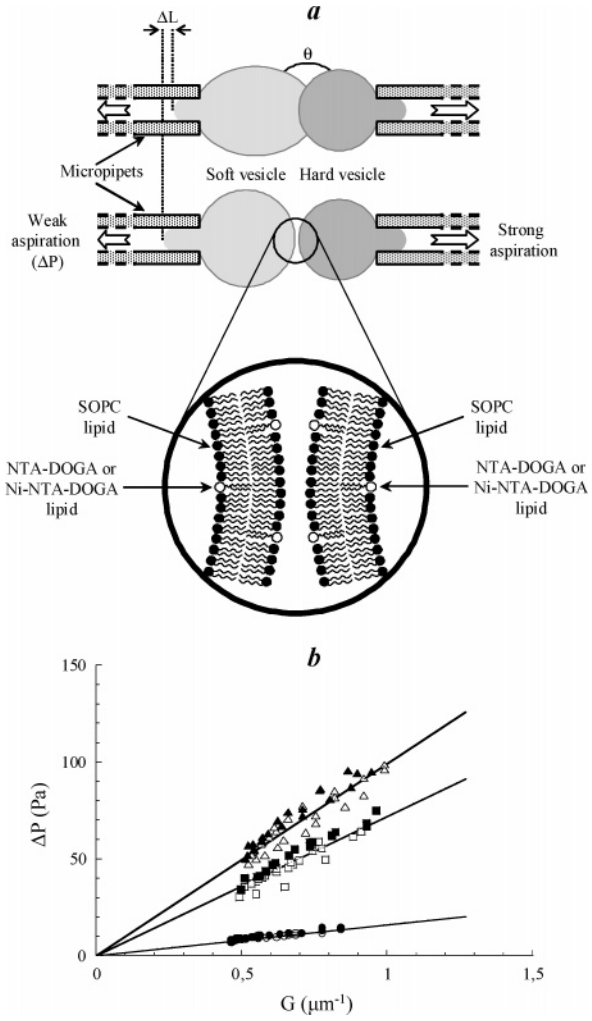

Figure 3. (a) Vesicle micromanipulation experiments. The adhesion energy (W_0) between the two vesicles is deduced from the deformation of the soft vesicle, characterized by a geometrical factor $G = 2(1 - Rc)/(1 - \cos\theta)R$ (see text). (b) Adhesion curves of the three systems (NTA/NTA, circles; NTA/Ni−NTA, squares; Ni−NTA/Ni−NTA, triangles; decreasing aspiration pressures, open symbols; increasing aspiration pressures, filled symbols). Adhesion energies (W_0) are given by the slope of the adhesion curves.

The force is measured with a leaf spring, and the distance is obtained interferometrically.[19] In the present paper, force measurements were made between two lipid bilayers deposited on silvered mica surfaces using the Langmuir−Blodgett deposition technique.[24] A first monolayer of DMPE lipid was deposited in a solid state, at 38 mN/m, with its headgroups on the mica surface. A second monolayer of NTA−DOGA or Ni−NTA−DOGA lipids was deposited in a fluid state, at 35 mN/m, with its headgroups facing the aqueous medium (Figure 2a). The reference distance $D = 0$ corresponds to the contact between DMPE hydrophobic tails. Force measurements were performed in a 10 mM Tris buffer (a minimal concentration of Tris buffer compatible with the pH control was used to minimize the probability of contamination of the surfaces to which the technique is very sensitive); they consisted of cycles of approaching and then separating the surfaces. For each case, at least three experiments and three cycles per experiment were made.

Vesicle Micromanipulation Technique. The vesicle micromanipulation technique gives the macroscopic adhesion energy per unit area between two free lipid bilayers. Two giant vesicles are aspirated by micropipets; one of the two vesicles is strongly aspirated (tight vesicle), and the other one is weakly aspirated (soft vesicle). The vesicles are then brought into contact. If an adhesion occurs, the soft vesicle deforms and takes the shape of the hard vesicle in the contact region (Figure 3a). The simultaneous knowledge of the geometrical parameters of this deformation (represented by a geometrical factor G) and of the aspiration pressure (ΔP) of the soft vesicle provides the adhesion energy per unit area (W_0) between the two vesicle membranes:[20−22]

$$W_0 = \frac{(1 - \cos\theta)R}{2(1 - Rc)}\Delta P = \frac{\Delta P}{G} \qquad (2)$$

where θ is the contact angle between the two vesicles; R is the radius of the micropipets, and c is the average curvature of the soft vesicle (Figure 3a). Assuming a constant vesicle area and volume, the two parameters c and θ can be calculated from the displacement (ΔL) of the soft vesicle inside its micropipet.[20] In practice, one first takes a picture of the two vesicles when they are far from each other in order to determine their initial geometrical parameters. Then, several aspiration pressures of the soft vesicle are tested in order to obtain good statistics and to probe the reversibility of the adhesion process. Only data from reversible adhesion processes are considered reliable.

Giant vesicles were formed by rehydration of a dried lipid film deposited on a roughened Teflon disk.[26,27] The lipid film was made of a 1:10 mixture in chloroform of NTA−DOGA or Ni−NTA−DOGA lipids and SOPC lipids (it was impossible to obtain stable giant vesicles from the pure NTA−DOGA or Ni−NTA−DOGA lipids). Vesicles were prepared in a 180 mM (190 mOsm) saccharose solution, and adhesion measurements were performed in a slightly hyperosmotic 130 mM (230 mOsm) Tris/NaCl buffer in order to have good osmotic control of the membrane tension.

Isothermal Titration Calorimetry (ITC). ITC is a convenient thermodynamic approach to monitor any chemical reaction initiated by the addition of binding components. By measuring the heat generated or absorbed during the association between interacting species, this method allows full determination of multiple thermodynamic parameters, such as the association constants (K), the reaction stoichiometry (n), the binding enthalpy (ΔH), and the entropy (ΔS).[23] In the present study, experiments were performed with an isothermal titration calorimeter from Microcal Inc.

In a typical experiment, the calorimetric cell was filled with 1.4 mL of a 0.05 mM solution of $NiCl_2$ in 100 mM Tris buffer (pH 8.0), and 5 μL aliquots of a 0.85 mM solution of NTA in 100 mM Tris buffer (pH 8.0) were successively injected (58 consecutive additions for a total volume of 290 μL of guest compound). The heat produced by the reaction was measured after each addition of NTA. The temperature (20 °C) was kept constant during the entire experiment, and continuous stirring was used to ensure rapid mixing of the solutions. Dilution effects were measured in a separate experiment by adding the same NTA solution to a pure Tris buffer solution. Thermodynamic and binding data were processed with the Microcal Origin software.

Results and Discussion

Force and Adhesion Measurements between Chelating Lipid Bilayers: Surface Characterization of the NTA−Ni−NTA Complex Binding Energy. The surfaces used in the SFA and the vesicle micromanipulation techniques contained either Ni−NTA−DOGA or NTA−DOGA lipids and were thus complexed or not with nickel ions (Ni−NTA and NTA surfaces, respectively). This leads to three experimental configurations for probing the molecular binding energy between Ni−NTA complexes and NTA groups: NTA/NTA, NTA/Ni−NTA, and Ni−NTA/Ni−NTA systems.

(25) Derjaguin, B. V.; Muller, V. M.; Toporov, Y. P. *J. Colloid Interface Sci.* **1975**, *53*, 314−326.
(26) Reeves, J. P.; Dowben, R. M. *J. Cell. Physiol.* **1969**, *73*, 49−60.
(27) Needham, D.; Evans, E. *Biochemistry* **1988**, *27*, 8261−8269.

Table 1. Average Adhesion Energies Deduced from Several SFA Experiments (E_0) and from Several Vesicle Micromanipulation Experiments (W_0)[a]

	F_0/R (mN/m)	F_e/R (mN/m)	F_{0eff}/R (mN/m)	E_0 (mJ/m^2)	W_0 (μJ/m^2)
NTA/NTA	-1 ± 1	12 ± 1	11 ± 2	1.8 ± 0.3	16 ± 3
NTA/Ni−NTA	4 ± 1	9 ± 1	13 ± 2	2.1 ± 0.3	72 ± 6
Ni−NTA/Ni−NTA	17 ± 1	7 ± 1	24 ± 2	3.8 ± 0.3	99 ± 6

[a] Effective separation force (F_{0eff}/R) is a corrected separation force, which takes into account the repulsive electrostatic interaction between the charged surfaces.

A typical result obtained for each experimental SFA configuration is given in Figure 2b. During the approaching phase, the three systems display similar features. Between 200 and 30 nm, no force is measured between the two surfaces. At 30 nm, a repulsive force sets in (inset in Figure 2b); this force is the electrostatic double-layer repulsion between two charged monolayers. In all cases, the decay length is 4 nm, which is close to the Debye length corresponding to a 10 mM Tris electrolyte. This electrostatic repulsion decreases when nickel ions are added to the monolayers (the charge is smaller when NTA groups are complexed with nickel ions). Below 8 nm, a steric repulsion is superposed on the electrostatic repulsion; this steric repulsion is due to the mobility of the headgroups that are linked to the hydrophobic tails through a flexible spacer.[28] The two monolayers come into contact at about 6 nm. As the zero reference distance is the one between the two DMPE monolayers on mica (as indicated in Figure 2a), this 6 nm distance corresponds to the thickness of two close-packed NTA−DOGA or Ni−NTA−DOGA hydrated monolayers. At the beginning of the separation process, there is no significant variation of the contact distance until, at a sufficient pulling force, the distance increases because of the stretching of the compressible parts of the lipid molecules (hydrophobic tails and flexible spacers). When the pulling force is equal to the adhesive force between the surfaces, which occurs when the distance increase is 2 nm, the two surfaces jump out of contact and end up far from each other (adhesive jump). Steric and electrostatic repulsive forces contribute to this pull-off force, F_0/R. To compare the different adhesive forces and to analyze them in terms of molecular bonds, one has to take into account the contribution of these repulsive forces. Since the adhesive jumps take place around 8 nm, the steric repulsion can be neglected. The force relevant to the contribution of the molecular bonds is thus an effective pull-off force, F_{0eff}/R, corresponding to the pull-off force that would be measured in the absence of the electrostatic double-layer repulsion, F_e/R:

$$\frac{F_{0\text{eff}}}{R} = \frac{F_0}{R} + \frac{F_e}{R} \tag{3}$$

where F_e/R is evaluated at the distance at which the adhesive jumps occur (Table 1).

The same three configurations have been studied with the vesicle micromanipulation technique. The adhesion curves are given in Figure 3b. These experiments directly provide adhesion energies and can be compared with the SFA results, where the effective pull-off force is proportional to the adhesion energy (eq 4 and Table 1).

Qualitatively, the same behavior was observed with SFA and vesicle micromanipulation techniques; increasing adhesion energies were respectively measured in the NTA/NTA, NTA/Ni−NTA, and Ni−NTA/Ni−NTA systems. The higher adhesion energy in the NTA/Ni−NTA case, relative to the NTA/NTA one, proves that adding nickel ions forms new bonds between the two surfaces. These new bonds can only be chelation bonds between NTA groups from one surface and nickel ions from the other, thus forming NTA−Ni−NTA complexes. The Ni−NTA/Ni−NTA system displays the highest adhesion energy. This is surprising since two NTA groups complexed with a nickel ion are not expected to form together any type of bond and, therefore, should lead to weaker adhesion energies. It has indeed been shown that when NTA surfaces are fully complexed with nickel ions, the adhesion is small.[5] This shows that in the present case, a certain amount of Ni−NTA groups lose their nickel ion in a Tris buffer. The ability of Tris molecules to capture nickel ions may explain this loss of nickel. The complexation constant of Tris molecules to metal ions, in general, and to nickel ions, in particular, is weak, but it will give a substantial effect if, as is the case here, the number of Tris molecules is 5 orders of magnitude larger than that of NTA molecules in the vicinity of the surfaces. For NTA/Ni−NTA and Ni−NTA/Ni−NTA systems, we thus observe an adhesive behavior due to the combined effect of interactions between NTA groups (whose origin is discussed in the Supporting Information) and chelation bonds between Ni−NTA complexes and NTA groups. The fact that the Ni−NTA/Ni−NTA system displays the highest adhesion energy reveals that less than 50% of the Ni−NTA groups still have their nickel ion in a Tris buffer. Indeed, in the case of a low proportion of NTA groups complexed with nickel ions, the Ni−NTA/Ni−NTA configuration displays the most favorable combination of chelation bonds.

From the adhesion energies measured for the three systems and using Boltzmann statistics, one can deduce the molecular binding energy between Ni−NTA complexes and NTA groups.

We first have to emphasize two established results. (i) The interaction energy between two Ni−NTA groups is weak enough to be within the error bar and can thus be neglected.[5] (ii) A certain proportion of Ni−NTA groups lose their nickel ion in the Tris buffer, as mentioned above. Thus, when facing an NTA group, they establish an NTA/NTA interaction, and when facing a Ni−NTA group, they form a chelation bond. Let us call p_{Ni} the proportion of Ni−NTA groups that still have their nickel ion.

Using these hypotheses, one can write adhesion energies measured in the three cases as the sum of two contributions, the first one corresponding to NTA/NTA interactions and the second one to chelation bonds.

In the case of SFA experiments, since no flattening of the surfaces was observed at contact, adhesion energies (E_0) are related to the effective separation forces between the two surfaces through the Derjaguin, Muller, and Toporov (DMT) relation:[25,29]

$$E_0 = \frac{F_{0\text{eff}}}{2\pi R} \tag{4}$$

(28) Kuhl, T. L.; Leckband, D. E.; Lasic, D. D.; Israelachvili, J. N. *Biophys. J.* **1994**, *66*, 1479−1488.

(29) Maugis, D. *J. Colloid Interface Sci.* **1992**, *150*, 243−269.

These adhesion energies can be written as

$$E_0(\text{NTA/NTA}) = E_{\text{NTA}} \quad (5)$$

$$E_0(\text{NTA/Ni}-\text{NTA}) = (1 - p_{\text{Ni}})E_{\text{NTA}} + p_{\text{Ni}}E_{\text{C}} \quad (6)$$

$$E_0(\text{Ni}-\text{NTA/Ni}-\text{NTA}) = (1 - p_{\text{Ni}})^2E_{\text{NTA}} + 2p_{\text{Ni}}(1 - p_{\text{Ni}})E_{\text{C}} \quad (7)$$

where E_{C} is equal to the adhesion energy that would be measured in the NTA/Ni−NTA case in a situation where all of the Ni−NTA groups still have their nickel ion.

Since each NTA group has one chelating site that can be either bound or unbound, E_{C} can be related to the microscopic binding energy (e_{C}) between one NTA group and one Ni−NTA group by Boltzmann statistics:

$$E_{\text{C}} = \Sigma_{\text{NTA}}\frac{e_{\text{C}}}{1 + \exp(-e_{\text{C}})} \quad (8)$$

where E_{C} and e_{C} are in $k_{\text{B}}T$ units, and where Σ_{NTA} is the surface density of chelating sites within their monolayer (from monolayer compression isotherms: $\Sigma_{\text{NTA}} = 1.89$ molecules·nm^{-2}).

Using eqs 5−8 and E_0 values given in Table 1, one can thus determine simultaneously p_{Ni} and e_{C}:

$$p_{\text{Ni}} = 0.15 \pm 0.05 \text{ and } e_{\text{C}} = 2.0 \pm 0.5,\ k_{\text{B}}T = 1.3 \pm 0.3 \text{ kcal/mol}$$

For vesicle micromanipulation experiments, one has to take the SOPC/SOPC interaction into account. This contribution, which is due to the van der Waals forces, has been evaluated in a separate experiment (adhesion measurement between two SOPC vesicles under the same experimental conditions; data not shown).

The adhesion energies (W_0) can be written as

$$W_0(\text{NTA/NTA}) - W_0(\text{SOPC/SOPC}) = W_{\text{NTA}} \quad (9)$$

$$W_0(\text{NTA/Ni}-\text{NTA}) - W_0(\text{SOPC/SOPC}) = (1 - p_{\text{Ni}})W_{\text{NTA}} + p_{\text{Ni}}W_{\text{C}} \quad (10)$$

$$W_0(\text{Ni}-\text{NTA/Ni}-\text{NTA}) - W_0(\text{SOPC/SOPC}) = (1 - p_{\text{Ni}})^2W_{\text{NTA}} + 2p_{\text{Ni}}(1 - p_{\text{Ni}})W_{\text{C}} \quad (11)$$

NTA−DOGA and Ni−NTA−DOGA lipids freely diffuse within the membrane of SOPC vesicles and are recruited into the contact region between the two vesicles. This leads to an enrichment of adhesion sites in the contact zone. A microcanonical description taking this enrichment into account has been developed and experimentally tested.[30] In the case of our systems, this leads to the relation

$$W_{\text{C}} = \frac{1}{10}\Sigma_{\text{NTA}}\left(\frac{\exp(e_{\text{C}}) - 1}{2}\right)k_{\text{B}}T \quad (12)$$

where the factor $^1/_{10}$ corresponds to the surface fraction actually covered by NTA groups (here, $\Sigma_{\text{NTA}} = 0.12$ molecules·nm^{-2}).

Using eqs 9−12 and W_0 values given in Table 1, we deduce

$$p_{\text{Ni}} = 0.25 \pm 0.10 \text{ and } e_{\text{C}} = 2.5 \pm 0.5,\ k_{\text{B}}T = 1.6 \pm 0.3 \text{ kcal/mol}$$

SFA and vesicle micromanipulation techniques give the same results. This validates the statistical approach and the use of both types of direct measurements. They both show that two NTA groups grafted on surfaces and facing each other can bind by sharing a nickel ion. This result has been suspected for a long time;[31] here, we prove it unambiguously and quantify the energy of the NTA−Ni−NTA bond.

Isothermal Titration Calorimetry: A Bulk Determination of Ni−NTA and NTA−Ni−NTA Complexes Binding Energies. Complementary microcalorimetry experiments have been performed to characterize the association in volume between one nickel ion and two NTA molecules and have compared it to results obtained with chelating lipid bilayers.

In a typical ITC experiment, the titration of a $NiCl_2$ solution was carried out with an NTA solution. Since nickel ions were in excess at the beginning of the titration and since adhesion experiments between chelating lipid bilayers showed that a Ni−NTA complex can bind a NTA molecule, complexation reactions occurred according to the following sequential pathway:

$$\text{Ni} + \text{NTA} \leftrightarrows \text{Ni}-\text{NTA}\ (K_1, e_1) \quad (13)$$

$$\text{Ni}-\text{NTA} + \text{NTA} \leftrightarrows \text{NTA}-\text{Ni}-\text{NTA}\ (K_2, e_2) \quad (14)$$

where K_i and e_i correspond, respectively, to the association constant and the binding energy of the reaction i. In this model, e_1 is the chelating energy of a nickel ion by an NTA group, and e_2 represents the binding energy of two NTA groups sharing a nickel ion, that is, the one measured in the previous section. Figure 4 displays the final experimental binding isotherm corresponding to the association of nickel ions and NTA molecules. The ITC fitting curve was obtained using a sequential binding site model (two binding sites), which gives access to both association constants, K_1 and K_2, and both binding energies, e_1 and e_2 (Table 2). We find that e_2 is 1.4 kcal/mol, which corresponds exactly to the one measured with SFA and vesicle micromanipulation experiments for NTA groups grafted on surfaces, and that e_1 is 6.5 kcal/mol. The corresponding dissociation constant (K_{D1}) of the Ni−NTA complex is in perfect agreement with the one previously measured on surfaces by impedance spectroscopy on thio−NTA monolayers and in bulk by fluorescence quenching or isothermal titration calorimetry.[32]

The success of this model confirms a posteriori the formation of both Ni−NTA and NTA−Ni−NTA complexes. It furthermore shows that the binding energy of the ternary NTA−Ni−NTA complex is about five times weaker than that of the binary Ni−NTA complex. We can assume that in the ternary complex, each NTA moiety binds the nickel ion through three bonds, whereas in the Ni−NTA complex, the nickel ion is trapped by the quadridentate NTA ligand in a cage structure fashion. The difference between the measured thermodynamic values e_1 and e_2 thus reflects the stabilization effect of the NTA cage.

(30) Pincet, F.; Perez, E.; Loudet, J. C.; Lebeau, L. *Phys. Rev. Lett.* **2001**, *8717*, 178101−178104.

(31) Schwarzenbach, G.; Biedermann, W. *Helv. Chim. Acta* **1948**, *31*, 331−340.

(32) Stora, T.; Hovius, R.; Dienes, Z.; Pachoud, M.; Vogel, H. *Langmuir* **1997**, *13*, 5211−5214.

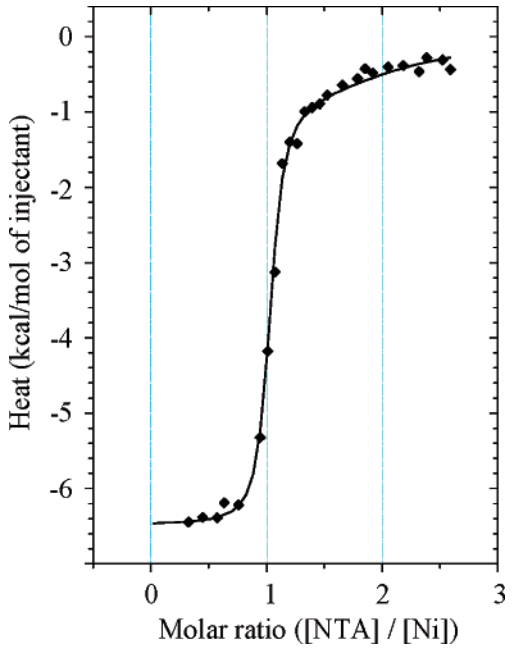

Figure 4. Isothermal titration calorimetry of a solution of $NiCl_2$ in 100 mM Tris buffer (pH 8) with NTA groups (heat of the reaction as a function of the molar ratio [NTA]/[Ni]). The curve is fitted by applying a sequential binding sites model (see text). The first part of the curve, up to 1 molar ratio, corresponds to the chelation of one nickel ion by one NTA molecule (nickel in excess). In the second part of the curve, the further addition of NTA molecules results in the formation of the ternary NTA−Ni−NTA complex.

Table 2. Association Constants (K_i), Dissociation Constants (K_{Di}), and Binding Energies (e_i) as Deduced from Isothermal Titration Calorimetry of Nickel Ions with NTA Molecules[a]

	microcalorimetry	other approaches
e_1 (or ΔH_1)	6.5 ± 0.1 kcal/mol	
K_1	1.8×10^7 M^{-1}	
K_{D1}	8.6×10^{-10} M	7.9×10^{-10} M[b]
e_2 (or ΔH_2)	1.4 ± 0.2 kcal/mol	1.3 ± 0.3 kcal/mol (SFA) 1.6 ± 0.3 kcal/mol (vesicle)
K_2	4.8×10^4 M^{-1}	
K_{D2}	3×10^{-7} M	

[a] K_{D1} and e_1 correspond to the chelation of a nickel ion by an NTA group. K_{D2} and e_2 are associated with the binding of two NTA groups sharing a nickel ion. Values of K_{Di} take into account the competition of amine protonation of the NTA moiety with complex formation. They are directly calculated from the association constants (K_i) computed by the Microcal Origin software using the following correction equation from ref 32: $K_{Di} = 10^{(pH - pK_a)}/K_i$, where $pK_a = 9.8$ and pH = 8.0. [b] From ref 32.

The Ni, Ni−NTA, and NTA−Ni−NTA species were also identified by UV absorption experiments (data not shown), which clearly showed that the formed complexes were the ones of the chemical reactions 13 and 14.

NTA−Ni−NTA complexes are very similar to His_2−Ni−NTA complexes, which are commonly used in protein purification methods. It can thus be speculated that their binding energies are of the same order (1−2 kcal/mol). This shows that the attachment of a protein to a Ni−NTA-coated surface through histidine is weak and, therefore, very labile. In most practical cases, the proteins to be separated are fused with a polyhistidine sequence, which strengthens the anchoring by a cooperativity effect.

Conclusion

A major goal in nanotechnology is the development of novel functional surfaces and supramolecular structures built upon the assembly of molecular blocks held together through weak interactions. Metal−ligand interactions have already been successfully used in order to generate complex molecular architectures with specific topology, high stability, and original properties.[3,33−36] The force and adhesion measurements obtained here in the technologically relevant context of chelating surfaces will be of fundamental importance for the fabrication of functional interfaces. Our results show that the stability of NTA−Ni−NTA complexes is not decreased when the interacting groups are grafted on surfaces, and that their corresponding binding energy, although weak, is significantly larger than the thermal energy, k_BT. Therefore, the sharing of a metal ion by two chelating agents offers a novel complexation mechanism that opens up a variety of avenues for the development of new supramolecular entities and anchoring strategies that are of major interest in the design of active interfaces with catalytic, sensing, or switching properties.

Supporting Information Available: The NTA/NTA interaction is characterized in terms of electrostatic forces and hydrogen bonds between the carboxyl functions of the NTA groups. This material is available free of charge via the Internet at http://pubs.acs.org.

JA043525Q

(33) Fujita, M. *Chem. Soc. Rev.* **1998**, *27*, 417−425.
(34) Semenov, A.; Spatz, J. P.; Moller, M.; Lehn, J. M.; Sell, B.; Schubert, D.; Weidl, C. H.; Schubert, U. S. *Angew. Chem., Int. Ed.* **1999**, *38*, 2547−2550.
(35) Holliday, B. J.; Mirkin, C. A. *Angew. Chem., Int. Ed.* **2001**, *40*, 2022−2043.
(36) Barth, J. V.; Weckesser, I.; Lin, N.; Dmitriev, A.; Kern, K. *Appl. Phys. A* **2003**, *76*, 645−652.